Nondipole Optical Scattering from Liquids and Nanoparticles

Natthi L. Sharma*

Department of Physics and Astronomy, Eastern Michigan University, Ypsilanti, Michigan 48197, USA

(Received 20 July 2006; published 24 May 2007)

Nondipolar contribution to optical scattering in liquids and nanoparticle suspensions has been discerned for the first time from the dominant electric dipole scattering by assigning the observed polarization and azimuthal angular distribution of scattered polarized light to *pure* magnetic dipole and/or electric quadrupole radiation and ruling out other (the impurity of laser polarization, multiple scattering, optical activity, and optical anisotropy) explanations. The observed scattering has potential use in the optical study of nanoparticles.

DOI: 10.1103/PhysRevLett.98.217402 PACS numbers: 78.67.Bf, 32.80.Fb, 42.68.Mj, 42.79.−e

It is known from electrostatics that a sphere in an initially uniform electric field is equivalent to a point electric dipole at its center for all external points. In scattering problems where the incident field is a plane wave which is neither uniform nor static, it is still possible to replace a spherical scatterer by an induced oscillating point electric dipole (ED) provided that the amplitude and phase of the incident wave does not change appreciably across the scatterer [1]. This latter stipulation, known as the (electric-)dipole approximation (DA), is realized when (a) the absorption is negligible and (b) the radius a of the scatterer and the inside wavelength λ satisfy $ka \ll 1$, where $k = 2\pi/\lambda$. In the scattering of light (*visible* radiation) from atoms, $(ka) \approx (v/c) \approx (Z/137)$, where Z is the atomic number [2]. Hence, excluding very high Z atoms, the DA is all that one needs to describe the light-atom interaction. For an extended source, a multipole expansion of interaction reduces it to a set of point multipoles with the contribution of successive terms decreasing as $(ka)^2$ [3].

Optical scattering measurements in atomic and molecular gases [4–6] and anisotropic liquids [7] have been adequately explained by isotropic and anisotropic response of scatterers using the DA. But in the $ka \sim 1$ range, the inclusion of the induced magnetic dipole (MD) contribution [8] has been shown to bring the accuracy of calculation closer to the exact results from Mie theory (Chapter 4, Ref. [1]). More recently, experimental and theoretical studies involving photoelectron emission by polarized x rays have confirmed the presence of electric quadrupole (EQ) and even higher multipole effects in the soft x-ray region [9–11]. This was somewhat expected because for soft (1 keV) x-ray photoionization of atoms $(ka) \approx 0.5$. In this Letter, I report the breakdown of the DA in the visible region—the very region for which it was invoked—but when the size or correlation length of scatterers is about 50 nm or more [12]. For example, we observe the presence of MD and/or EQ induced scattering of light from nanoparticle suspensions ($ka \geq 0.3$) and even from molecular liquids. This breakdown of the DA in the visible region was recognized by observing the polarization and angular distribution of scattered light in the transverse plane, the plane perpendicular to the incident polarized laser beam, as shown in Fig. 1. In the transverse plane, apart from the ED scattering induced by the electric field of the incident light (upper curves in Figs. 2–5) with its $\sin^2\phi$ angular distribution and transverse (perpendicular to $\mathbf{k}$ and parallel to $\hat{\boldsymbol{\phi}}$) polarization, a small fraction of scattered light was observed (lower curves in Figs. 2–5) to have a $\cos^2\phi$ angular distribution and axial (parallel to $\mathbf{k}$) polarization. Based on the theoretical analysis that follows, the latter radiation with axial polarization is recognized either as the magnetic dipole radiation produced by the magnetization induced in the target by the magnetic field of the incident light or as the induced quadrupole radiation driven by the electric field gradient that exists along the direction of propagation of the incident light or a superposition of both of the above. This MD-EQ scattering could be exploited to determine the size of nanoparticles in suspensions, such as colloids and atmospheric aerosols.

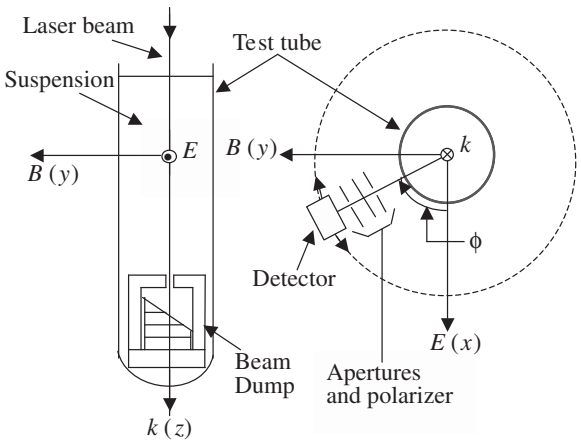

FIG. 1. An x-polarized laser beam from a 10 mW He-Ne laser travels vertically down along the axis of a test tube containing the liquid specimen. In this transverse scattering geometry, the angular distribution of scattered light is measured in the xy plane, the plane transverse to the incident beam, as a function of azimuthal angle ϕ. The beam is dumped into a cavity to eliminate retroreflection and spurious light.

The angular distribution of the scattered radiation is governed by the coherent superposition of fields generated by the electric and magnetic multipoles induced in the scatterers by the incident radiation. When we go beyond the DA, we retain both the MD and the EQ terms because they happen to be of the same order [2]. Choosing the origin of coordinates inside the scatterer, the electric field of the scattered radiation $\mathbf{E}_{\rm sc}$ at vector position $\mathbf{r} = r\hat{\mathbf{r}}$ is given by [13]

$$\mathbf{E}_{\rm sc}(\mathbf{r},t) = -\frac{\mu_o \omega^2 e^{ikr}}{4\pi r} \times \left[\hat{\mathbf{r}}\times(\hat{\mathbf{r}}\times\mathbf{p}) + \frac{1}{c}\hat{\mathbf{r}}\times\mathbf{m} - i\frac{\omega}{6c}\hat{\mathbf{r}}\times(\hat{\mathbf{r}}\times\mathbf{Q})\right], \quad (1)$$

where $\mathbf{p}$ and $\mathbf{m}$ are the electric and magnetic dipole moments, respectively, and the vector $\mathbf{Q}$, which is related to the quadrupole moment tensor $Q_{ij} \equiv \int(3r_i r_j - r^2\delta_{ij})\rho(\mathbf{r})d^3r$ through $Q_i = \sum_j Q_{ij}(r_j/r)$, depends on the direction of observation. The multipole moments induced in an *isotropic* scatterer at the origin by an incident plane wave, $\mathbf{E}_{\rm inc} = \hat{\mathbf{x}}E_0\exp[-i\omega(t - z/c)]$, are, respectively, given by [14]

$$\mathbf{p}(t) = \hat{\mathbf{x}}\alpha_e E_0 e^{-i\omega t}, \qquad \mathbf{m}(t) = \alpha_m \mathbf{B}_{\rm inc}(t) = \hat{\mathbf{y}}\alpha_m (E_0/c)e^{-i\omega t}, \quad (2)$$

$$\mathbf{Q}(t) = Q_{zx}\left(\frac{z}{r}\hat{\mathbf{x}} + \frac{x}{r}\hat{\mathbf{z}}\right) \equiv \left(\frac{z}{r}\hat{\mathbf{x}} + \frac{x}{r}\hat{\mathbf{z}}\right)\alpha_Q E_0 e^{-i\omega t}, \quad (3)$$

where α_e, α_m, and α_Q are, respectively, the induced electric, diamagnetic, and quadrupole polarizabilities of the scatterers [15]. There is only an electronic contribution to α_e because there are no ionic or orientational contributions at visible frequencies. Similarly, there is only an orbital contribution (no spin contribution) to α_m. Since the incident electric field has a nonvanishing gradient only along the z direction, the direction of propagation, only $Q_{zx} \equiv Q_{xz}$ is nonzero. Substitution of $\mathbf{p}$, $\mathbf{m}$, and $\mathbf{Q}$ from Eqs. (2) and (3) into Eq. (1), yields

$$\mathbf{E}_{\rm sc}(r,\theta,\phi) = -\frac{\mu_o\omega^2}{4\pi r}E_o e^{ikr}\left[\left\{\alpha_e + \left(\frac{\alpha_m}{c^2} - \frac{i\omega\alpha_Q}{6c}\right)\cos\theta\right\} \times (\sin\phi\hat{\boldsymbol{\phi}}) - \left\{\alpha_e\cos\theta + \frac{\alpha_m}{c^2} - \frac{i\omega\alpha_Q}{6c} \times \cos 2\theta\right\}(\cos\phi\hat{\boldsymbol{\theta}})\right]. \quad (4)$$

The angular dependence of various terms in $\mathbf{E}_{\rm sc}$ above agrees with that obtained by retaining the ED, MD, and EQ terms in the multipole series due to Mie (p. 94, Ref. [1]). For scattering measurements in the transverse xy plane (see Fig. 1), $\theta = \pi/2$ and $\hat{\boldsymbol{\theta}} = -\hat{\mathbf{z}} = -\hat{\mathbf{k}}$, the ED part of $\mathbf{E}_{\rm sc}$ (which is now purely along $\hat{\boldsymbol{\phi}}$) becomes perpendicular to the MD and EQ fields both of which are now polarized along $\hat{z}$ and can therefore be filtered using a polarizer. The corresponding filtered intensities for *isotropic* scatterers, obtained with $\theta = \pi/2$ in Eq. (4) and multiplying the ϕ and the z components of $\mathbf{E}_{\rm sc}$ by their respective complex conjugates, are [16]

$$I_\phi(\phi) = I_{\rm inc}\frac{\mu_o^2\omega^4}{16\pi^2 r^2}\alpha_e^2\sin^2\phi \qquad [\text{Transverse}] \quad (5)$$

$$I_z(\phi) = I_{\rm inc}\frac{\mu_o^2\omega^4}{16\pi^2 r^2}\left[\frac{\alpha_m^2}{c^4} + \frac{\omega^2\alpha_Q^2}{36c^2}\right]\cos^2\phi, \quad [\text{Axial}], \quad (6)$$

where $I_{\rm inc} = (1/2)\epsilon_o c E_o^2$ is the intensity of the incident light. In going from Eq. (4)–(6), we have taken the polarizabilities α_e, α_m, and α_Q to be real, which is justifiable for dielectric liquids and aqueous suspensions of dielectric nanoparticles. For a random distribution of scatterers in a suspension, since the scattering is incoherent, the intensities I_ϕ and I_z get multiplied by the number of scatterers in the region of the beam exposed to the detector. For transparent liquids, such as carbon tetrachloride (CCl_4) and benzene (C_6H_6) in Figs. 2 and 3, the lateral scattering is expected to be small because of constructive interference (coherent scattering) in the forward direction but not zero.

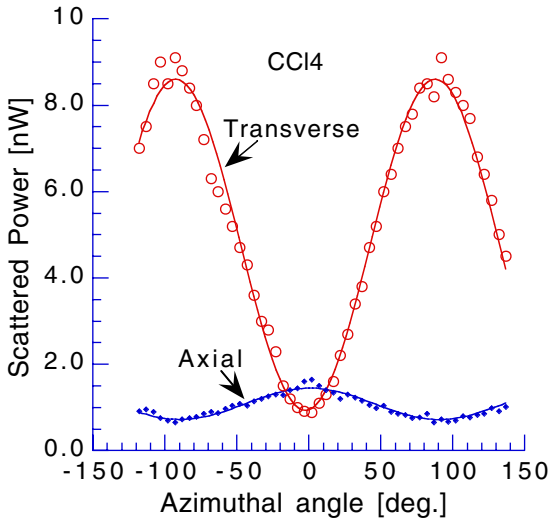

FIG. 2 (color online). Angular scattering of polarized light in 99.9% pure CCl_4, an isotropic liquid scatterer. "Transverse" (axial) refers to scattered power measured with a horizontal (vertical) polarizer in front of the detector. The symbols represent measurements and the solid curves represent fits of the function $A + B\sin^2\phi$ to the data. The minimum of the transverse curve is found to coincide with the direction of polarization of the laser beam. As expected, the lateral scattering is small in pure transparent liquids. The nondipole contribution is 12.5% of the ED contribution. This is the percentage ratio, R, of peak-to-valley differences of axial and transverse signals. Fluctuations in the CCl_4 data are because of formation of tiny bubbles in the path of the laser beam; we recorded the lowest reading each time. Scattering from distilled water was found to be very similar to the CCl_4 data and in the same range.

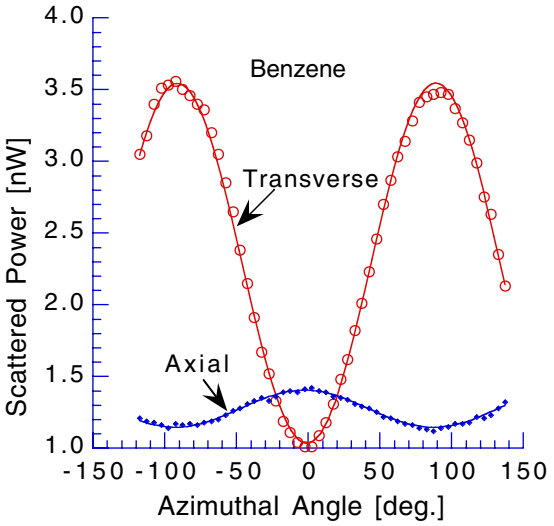

FIG. 3 (color online). Azimuthal angular distribution of scattered light from liquid benzene. Here $R = 10.5\%$. As compared to CCl_4, the offset for the axial curve for benzene is higher because of the molecular anisotropy contribution via the induced ED moment $\alpha_{zx}E_x$.

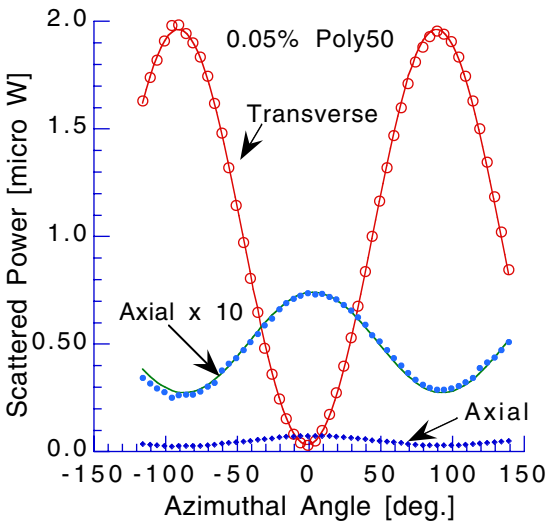

FIG. 4 (color online). Azimuthal angular distribution of light scattered from a 0.05% aqueous suspension of 46 ± 7 nm diameter polystyrene spheres. The actual axial data (shown at the bottom) is multiplied by 10 to clearly show the angular variation and curve fitting. $R = 2.5\%$.

Taking the MD and EQ terms in Eq. (6) of the same order, the ratio of axial to transverse intensities is

$$\left(\frac{I_z}{I_\phi}\right)_{\max} \approx \frac{\alpha_m^2}{c^4\alpha_e^2} = \frac{m^2}{c^2p^2}. \tag{7}$$

In the limiting case of a perfectly conducting spherical scatterer of radius a, with $\alpha_e = 4\pi\epsilon_0 a^3$ and $\alpha_m = -2\pi a^3/\mu_0$ [13], this ratio is $1/4$ and it is expected to be smaller for dielectric scatterers.

Measurements of angular distribution (Figs. 2–5) in the transverse plane, with a horizontal (transverse) and vertical (axial) polarizer before the detector, agree very well with Eq. (5) and (6), respectively. Experimentally, we define the relative strength of the nondipole contribution as the percentage polarization ratio, R, of peak-to-valley differences of axial and transverse signals. The measured R values in Figs. 2–5 lie between 2%–13%, also in agreement with the expectation of less than 25% for a perfectly conducting sphere from Eq. (7). The agreement between observed and calculated angular distributions is true not only for isotropic scatterers like CCl_4 and polystyrene spheres, but even for benzene and other anisotropic scatterers, e.g., silver chloride [17]. This separation of axial MD-EQ scattering from the dominant transverse ED scattering is possible *only* in the transverse ($\theta = \pi/2$) scattering geometry of Fig. 1. In addition, many difficulties encountered in the commonly used beam-plane scattering geometry [4,7] with a *horizontal* laser beam (e.g., the forward-backward asymmetry due to beam divergence, the angular dependence of interaction volume between the laser beam and scatterers, and the change in reflectivity and polarization of the scattered light when passing through the walls of scattering chamber at oblique angles) were eliminated here. It is not possible (though they differ in parity), however, to further separate the MD from the EQ scattering if both are present.

Our conclusion of the presence of MD-EQ scattering is further strengthened because the following other scenarios can not account for the axial (scattered) electric field with a $\cos\phi$ angular dependence. The vertical laser beam does not

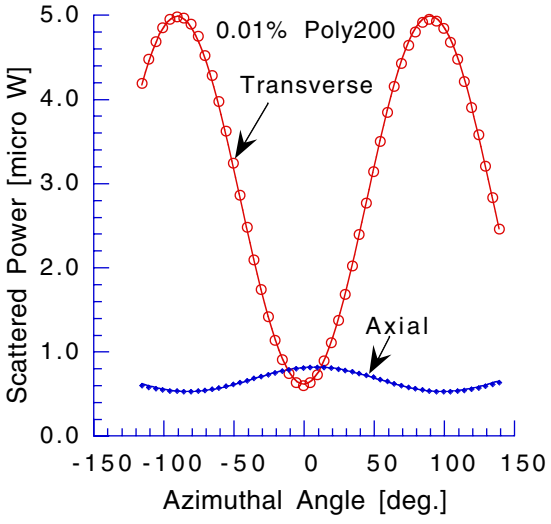

FIG. 5 (color online). Azimuthal angular distribution of light scattered from a 0.01% aqueous suspension of 194 ± 8-nm diameter polystyrene spheres. The scattering concentration was decreased by a factor of 5 as compared to 46-nm diameter polysterene suspension to preserve the clarity of the suspension from increased background scattering from higher multipoles for larger particles. $R = 7\%$, about $\frac{(194/46)^2}{5}$ times bigger compared to 46-nm polystyrene spheres.

have any vertical (axial) electric field. Even if it did, the scattered vertical E field in the transverse plane will have no angular variation. The y polarization of the laser beam, if any (<1 in 500), would generate transverse, not axial, polarization of the scattered light. Multiple scattering, though small in dilute suspensions, will certainly generate some axially polarized background (part of the offset seen in ''axial'' curves), but there is no reason for it to have a $\cos^2\phi$ angular dependence. Though our scatterers are achiral, even in chiral ones, an incident E field in the x direction can induce a magnetic moment in the x direction, which in turn can generate an axial E field in the xy plane, but with a $\sin\phi$ (not $\cos\phi$) angular distribution.

Anisotropy in the ED response of scatterers adds $\alpha_{yx}\hat{\mathbf{y}}$ and $\alpha_{zx}\hat{\mathbf{z}}$ to $\alpha_e\hat{\mathbf{x}}$ in $\mathbf{p}$ in Eq. (2), where α_{yx} and α_{zx} are components of the ED polarizability tensor. We have used α_e for the diagonal component α_{xx}. These extra terms in $\mathbf{p}$ add, assuming real α's, a *first order* correction term proportional to $-\alpha_e\alpha_{yx}\sin 2\phi$ to I_ϕ and a term proportional to $\alpha_{zx}^2 - 2(\alpha_m\alpha_{zx}/c^2)\cos\phi$ to I_z [17]. For isotropic scatterers such as CCl_4 and polystyrene spheres these added terms are zero because α_{yx} and α_{zx} are zero. Even for anisotropic scatterers such as benzene and silver chloride [17] suspension, these *interference* terms (terms with two different α's) vanish when $\mathbf{p}$ is summed over random orientations of scatterers in the scattering region [18].

In summary, the observed axially polarized scattered light with a $\cos^2\phi$ angular variation in the azimuthal plane is produced by *pure* MD and/or EQ scattering. We do not observe ED-MD and/or ED-EQ interference effects because of isotropy of scatterers or their random orientations in liquids. In *inelastic* x-ray studies [9–11], the MD contribution was forbidden [19] even when EQ and higher multipole effects were present. In the *elastic* scattering studied here, both MD and EQ scattering are allowed but not separable. With lasers of higher power and frequency (MD and EQ scattering are $\propto\omega^4$ and ω^6, respectively) these measurements could be used to study atmospheric aerosols and nanoparticle suspensions in plasmas [6,20]. Besides the data on liquids and isotropic dielectric scatterers presented here, measurements on colloidal suspensions of silver chloride and skim milk show similar results [17]. The latter could be of relevance in colloidal chemistry. More importantly, the MD-EQ optical scattering from nanoparticles may be useful for size determination [21] of nanoparticles in rapidly emerging nanotechnologies [22].

The author is grateful to Ernest Behringer for his help with figures and discussion.

Note added in proof.—Inspired by this work, a nonlinear version of MD scattering has just been reported [23].

*Electronic address: nsharma@emich.edu

[1] C. F. Bohren and D. R. Huffman, *Absorption and Scattering of Light by Small Particles* (Wiley-Interscience, New York, 1983), Section 5.2; H. C. van de Hulst, *Light Scattering by Small Particles* (Dover, New York, 1981), Chap. 9.
[2] H. A. Bethe and E. E. Salpeter, *Quantum Mechanics of One- and Two-Electron Atoms* (Plenum, New York, 1977), Sec. 59 and 66.
[3] J. M. Blatt and V. F. Weisskopf, *Theoretical Nuclear Physics* (Wiley, New York, 1952), p. 592.
[4] T. V. George *et al.*, Phys. Rev. Lett. **11**, 403 (1963); Phys. Rev. **137**, A369 (1965).
[5] R. D. Watson and Maynard K. Clark, Phys. Rev. Lett. **14**, 1057 (1965).
[6] R. F. G. Meulenbroeks, D. C. Schram, L. J. M. Jaegers, and M. C. M. van de Sanden, Phys. Rev. Lett. **69**, 1379 (1992).
[7] R. C. C. Leite, R. S. Moore, S. P. S. Porto, and J. E. Ripper, Phys. Rev. Lett. **14**, 7 (1965).
[8] G. W. Mulholland, C. F. Bohren, and K. A. Fuller, Langmuir **10**, 2533 (1994).
[9] B. Krassig, M. Jung, D. S. Gemmell, E. P. Kanter, T. LeBrun, S. H. Southworth, and L. Young, Phys. Rev. Lett. **75**, 4736 (1995).
[10] A. Derevianko, O. Hemmers, S. Oblad, P. Glans, H. Wang, S. B. Whitfield, R. Wehlitz, I. A. Sellin, W. R. Johnson, and D. W. Lindle, Phys. Rev. Lett. **84**, 2116 (2000).
[11] O. Hemmers *et al.*, Phys. Rev. Lett. **91**, 053002 (2003).
[12] A low frequency analogy is television (UHF) reception where with a as the antenna size, $ka \sim 1$, and the MD and ED terms are comparable, justifying the replacement of an electric dipole rabbit-ear antenna with a magnetic loop antenna.
[13] John D. Jackson, *Classical Electrodynamics* (Wiley, New York, 1999), 3rd ed., pp. 414, 457.
[14] L. D. Barron, *Molecular Light Scattering and Optical Activity* (Cambridge University Press, Cambridge, England, 2004) Chap. 3.
[15] For transparent materials where atomic resonance frequencies $\hat{\omega}_o$ are in the ultraviolet region and absorption is negligible, $\alpha_e = e^2/m(\hat{\omega}_o^2 - \hat{\omega}^2)$ and $\alpha_m = -e^2\langle r^2\rangle/6m$, where e and m are the charge and mass of an electron, and $\langle\ldots\rangle$ stands for the expectation value. See, for example, R. P. Feynman, R. B. Leighton, and M. Sands, *The Feynman Lectures on Physics* (Addison-Wesley, Reading, 1964), Vol. 2, pp. 32-2 and 34-6.
[16] For a quantum calculation, see: W. R. Johnson and F. D. Feiock, Phys. Rev. **168**, 22 (1968).
[17] Data on colloidal suspensions and full details of analysis will be published elsewhere.
[18] A. C. Holland and G. Gagne, Appl. Opt. **9**, 1113 (1970); J. C. Tully, R. S. Berry, and B. J. Dalton, Phys. Rev. **176**, 95 (1968).
[19] J. W. Cooper, Phys. Rev. A **47**, 1841 (1993).
[20] G. Gebauer and J. Winter, New J. Phys. **5**, 38 (2003).
[21] M. Kerker and M. I. Hampton, J. Opt. Soc. Am. **43**, 370 (1953).
[22] M. Taneike *et al.*, Nature (London) **424**, 294 (2003).
[23] S. L. Oliveira and S. C. Rand, Phys. Rev. Lett. **98**, 093901 (2007).